Available online at www.sciencedirect.com
SCIENCE DIRECT
Journal of Photochemistry and Photobiology A: Chemistry 181 (2006) 268–273
Journal of Photochemistry and Photobiology A:Chemistry
www.elsevier.com/locate/jphotochem

Theoretical studies of 1:1 charge-transfer complexes between nitrogen-containing heterocycles and I_2 molecules, and implications on the performance of dye-sensitized solar cell

Hitoshi Kusama *, Hideki Sugihara

Energy Technology Research Institute, National Institute of Advanced Industrial Science and Technology (AIST), AIST Tsukuba Central 5, 1-1-1 Higashi, Tsukuba, Ibaraki 305-8565, Japan

Received 7 September 2005; received in revised form 30 November 2005; accepted 5 December 2005
Available online 18 January 2006

Abstract

Ab initio molecular orbital (MO) methods were used to examine the monomer and intermolecular charge-transfer 1:1 complexes of six different nitrogen-containing heterocycles with I_2. The calculations at the MP2(full)/LANL2DZ* levels in acetonitrile revealed that the σ* orbital of diiodine interacts with the N lone pair in the heterocyclic ring. The open-circuit photovoltage (V_{oc}) values of a Ru(II) complex dye-sensitized nanocrystalline TiO_2 solar cell with an I^-/I_3^- redox electrolyte in acetonitrile using N-containing heterocyclic additives were compared to the computational calculations of the intermolecular interaction between the heterocycles and I_2. The Gibbs free energy changes, optimized geometries, frequency analyses, Mulliken population analyses, and natural bond orbital (NBO) analyses indicated that the V_{oc} value of the solar cell is higher when the N-containing heterocyclic compounds have a stronger interaction with I_2. In addition, the V_{oc} increases as the energy of the HOMO level increases and becomes closer to the LUMO level of the I_2 molecule. Therefore, the intermolecular charge-transfer interaction between the heterocyclic additives and the iodine redox electrolyte is an important factor for dominating dye-sensitized solar cell performance.

Keywords: Nitrogen-containing heterocycles; Iodine; Charge-transfer complex; Dye-sensitized solar cell

1. Introduction

A typical dye-sensitized solar cell, illustrated in Fig. 1, consists of a nanocrystalline TiO_2 film photoelectrode covered with a sensitizing dye such as a Ru(II) complex, a redox electrolyte like I^-/I_3^-, and a counter electrode such as Pt. This type of solar cell has been intensively studied since Grätzel reported a very high solar energy conversion efficiency (η) [1]. One method for improving solar cell performance is to add organic bases to the electrolyte solution. For example, Frank and co-workers studied an I^-/I_3^- electrolyte with ammonia and 4-*t*-butylpyridine as additives in acetonitrile and reported that these additives drastically increased both the V_{oc} and η [2,3]. Based on these findings, we examined the effects of five- and six-membered N-containing heterocycles as additives in an I^-/I_3^- redox electrolyte in acetonitrile on the $(dcbpy)_2Ru(SCN)_2{\cdot}2TBA$ (dcbpy: 2,2′-bipyridine-4,4′-dicarboxylic acid, TBA: tetrabutylammonium, N719) dye-sensitized TiO_2 solar cell performance. Consequently, we determined that these heterocycles significantly influenced the performance of the cell. Most of the N-containing heterocycles enhanced the V_{oc} of the solar cell and semi-empirical MO calculations indicated that the V_{oc} increased as the ionization energy of the heterocycles molecules decreased [4]. This finding is explained by a charge-transfer (or electron donor–acceptor) complexation between the heterocycles and iodine. The chemical equilibrium in the electrolyte solution is written as Eq. (1):

$$\text{Heterocycles} + I_3^- \rightleftarrows \text{Heterocycles}\,I_2 + I^- \quad (1)$$

This reaction reduces the I_3^- concentration, $[I_3^-]$, but increases the I^- concentration, $[I^-]$, which increases the hole collection by

* Corresponding author. Tel.: +81 29 861 4867; fax: +81 29 861 6771.
E-mail address: h.kusama@aist.go.jp (H. Kusama).

1010-6030/$ – see front matter © 2005 Elsevier B.V. All rights reserved.
doi:10.1016/j.jphotochem.2005.12.008

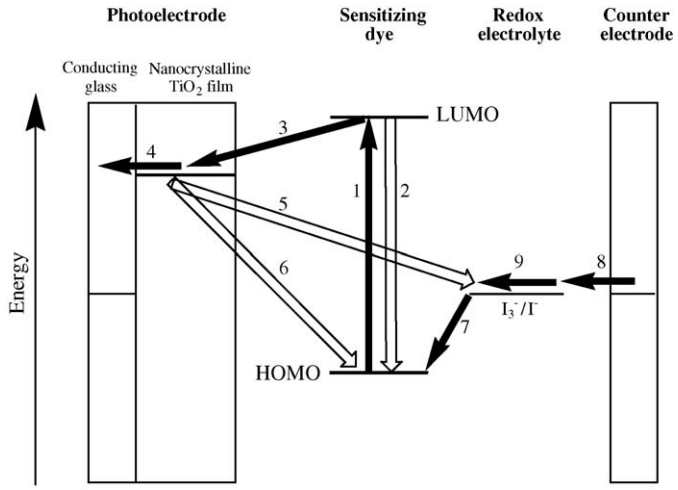

Fig. 1. Schematic description of the charge transfer in a dye-sensitized solar cell. (1) Excitation of the dye; (2) excited dye decay to ground; (3) electron injection; (4) electron transport and collection at the conducting glass; (5) recombination of the electron with electrolyte; (6) recombination of the electron with oxidized dye; (7) reduction of the oxidized dye by I^- ions to regenerate the original one (I^- oxidation); (8) I_3^- reduction; and (9) ion transport.

I^- [5,6] and improves the V_{oc} of the solar cell. Reducing the $[I_3^-]$ may also decrease the reaction between the injected electrons and I_3^- at the semiconductor electrolyte junction (Eq. (2)). That is, the electrons recombine with the electrolyte in Fig. 1(5).

$$2e_{cb}^-(TiO_2) + I_3^- \xrightarrow{k_{et}[I_3^-]} 3I^- \quad (2)$$

This would elevate the electron concentration in the TiO_2 film and enhance the V_{oc} value (Eq. (3)) [2,6],

$$V_{oc} = \left(\frac{kT}{e}\right) \ln\left(\frac{I_{inj}}{n_{cb}k_{et}[I_3^-]}\right) \quad (3)$$

where k and T are the Boltzmann constant and the absolute temperature, respectively. I_{inj} is the charge flux due to the sensitizing dye injecting an electron (Fig. 1(3)) and n_{cb} is the concentration of electrons at the TiO_2 surface, while k_{et} is the rate constant for the reduction of I_3^- by the conduction band electrons. As the $[I_3^-]$ and/or k_{et} decreases in Eq. (3), the V_{oc} increases [2,7].

Eq. (4) is a simplified form of the intermolecular charge-transfer 1:1 complexation.

$$\text{Heterocycles} + I_2 \rightarrow \text{Heterocycles}\,I_2 \quad (4)$$

The interaction between the HOMO of the donors (N-containing heterocycles) and the LUMO of the acceptors (I_2) explains the theory [8]. The greater the overlap and/or the smaller energy difference of the HOMO of the donor and the LUMO of acceptor, the larger the stabilization energy, Δ, and the greater the extent of mixing, which causes more charge transfer from the donor to the acceptor. Thus, it is easier to form a charge-transfer complex when the ionization energy of the donor is small and the electron affinity of the acceptor is large. Therefore, the lower the ionization energy of the heterocycles, the more efficiently the holes are collected and/or the electron concentration in the TiO_2 film increases, which results in a higher V_{oc} [4].

Although the ionization energy of the N-containing heterocycles is an index for intermolecular charge-transfer complexation with I_2, a detailed understanding of complexation such as the intermolecular N···I atom distances, which involve electron transfer from the nitrogen donor lone pair (n) of the heterocyclic ring to the antibonding molecular orbital σ* of diiodine to form n–σ complexes [9–11] and so on, is lacking. The formation of charge-transfer complexes has been reported, but experimental data using spectroscopic methods such as UV–vis are not sufficiently present in the literature [9,10]. However, it is possible to analyze the complexation of N-containing heterocycles with I_2. To aid in the understanding of intermolecular charge-transfer complexation, computational calculations have been attempted on pyridine with I_2 [12–14]. To the best of our knowledge, theoretical computational studies on an intermolecular complex of other six-membered N-containing heterocycles (azines) and five-membered ones (azoles) with I_2 have yet to be reported. An ab initio MO method with optimized geometries was used to investigate the 1:1 charge-transfer interaction between six types of N-containing heterocycles, which enhanced the V_{oc} of Ru(II) complex dye-sensitized solar cell, and I_2. The aim of the present work is to identify the intermolecular charge-transfer interaction properties of N-containing heterocycles·I_2 and to confirm the correlation between the V_{oc} of the solar cell and the complex properties.

2. Computational details

All ab initio MO calculations were performed using the Gaussian 03 W program [15] on personal computers. The complex and monomer geometries were fully optimized at the second-order Moller–Plesset (MP2, full) levels. For all systems, a LANL2DZ* basis set, which includes an effective core potential (ECP) for all atoms except for the first row [16], was used. Hay and Wadt proposed the ECP used [17–19] in which the iodine incorporates the mass velocity and Darwin relativistic effects. The LANL2DZ basis set corresponds to a Dunning/Huzinaga full double-ζ basis (D95) [20] for the first-row elements and an ECP plus double-ζ basis for the iodine atoms [21]. This basis set was augmented with one set of six d polarization function (LANL2DZ*) with the following exponents: $\alpha_C = \alpha_N = 0.8$, and $\alpha_I = 0.29$ [22,23]. Recently, this basis set was shown to yield reasonable results for I_2 complexes with pyridine [14], thiocarbonyl derivatives [24], and lactams [25]. The harmonic vibrational frequencies confirmed that the optimized structures correspond to real minima on the potential energy surface [26].

The solvent effects of acetonitrile were modeled using an integral equation formalism (IEF) polarized continuum model (PCM) of Tomasi et al. [23,27,28] within the self-consistent reaction field (SCRF) theory. In the SCRF calculations, the dielectric constant ε of acetonitrile was 36.64.

To understand the nature and magnitude of the intermolecular interactions, NBO analysis [21,29] was conducted on the optimized geometries using the NBO 3.1 program [30], which is included in the Gaussian package program.

Table 1
The influence of the N-containing heterocycles in the I^-/I_3^- redox electrolyte solution on the open-circuit photovoltage (V_{oc}) in a dye-sensitized solar cell

No.	Heterocycles	V_{oc} (V)
	None	0.620
a	Pyrazole	0.674
b	Imidazole	0.848
c	1,2,4-Triazole	0.692
d	Pyridine	0.730
e	Pyrimidine	0.666
f	Pyrazine	0.672

Conditions: electrolyte, 0.6 mol/dm^3 1,2-dimethyl-3-propylimidazolium iodide +0.1 mol/dm^3 LiI +0.05 mol/dm^3 I_2 +0.5 mol/dm^3 additive in acetonitrile; light intensity, 100 mW/cm^2, AM 1.5.

3. Results and discussion

3.1. Correlation between the V_{oc} and the theoretical calculation of isolated molecules

Table 1 lists the N-containing heterocyclic compounds and the previous V_{oc} results [4] that are used in this work. Fig. 2 depicts the correlation between the V_{oc} and the calculated energy of the HOMO level for the heterocyclic monomers. The V_{oc} increases as the energy of the HOMO level increases and becomes closer to the LUMO level of the I_2 molecule (−0.01456 a.u.). As mentioned in Section 1, the smaller the energy difference between the HOMO of the donor and the LUMO of acceptor, the greater the charge transfer from the donor to the acceptor and the easier a charge-transfer complex is formed. Thus, this correlation confirms that a higher V_{oc} occurs when a more efficient charge-transfer complex between heterocyclic compounds and I_2 is formed. As previously reported, the energy of the HOMO level for the heterocycles obtained in this study becomes more negative as the ionization energy increases [4].

3.2. Correlations between the V_{oc} and the theoretical calculations of the complexes

Fig. 3 shows the correlation between the V_{oc} and the Gibbs free energy changes (ΔG) for Eq. (1). Negative ΔG values were observed for all the molecules. A negative ΔG implies that the equilibrium of Eq. (1) shifts to the right, which provides the initial evidence that all the tested N-containing heterocycles form intermolecular charge-transfer complexes with I_2. The more negative the ΔG value, the more favorable the right side of the equilibrium in Eq. (1) is, which results in more complexation. Thus, the correlation where the V_{oc} increases as the ΔG value becomes more negative confirms that a higher V_{oc} occurs when a more efficient charge-transfer complex is formed between heterocyclic compounds and I_2.

Fig. 4 illustrates the optimized molecular structures for the 1:1 heterocycle·I_2 complexes, which show the most significant structure parameters. Compared to the I_2 monomer (2.6979 Å), all the intramolecular I1–I2 bonds in the complexes are elongated, indicating that the I_2 monomer bond is weakened. The forming intermolecular N···I1 σ-bonds are shorter than

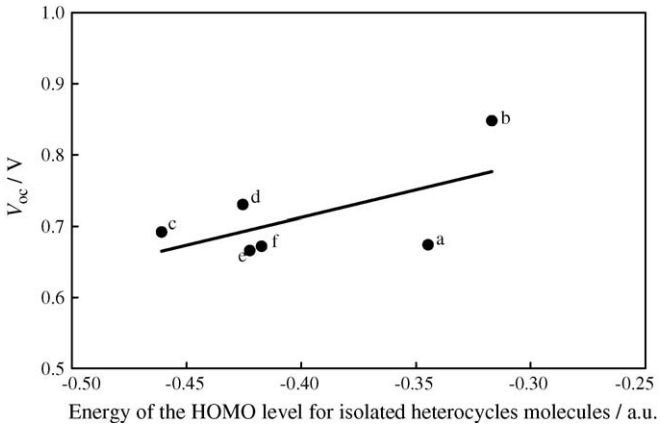

Fig. 2. Correlation between the V_{oc} and the energy of the HOMO level for the isolated N-containing heterocycles molecules. The number of each heterocycles is defined in Table 1.

the sum of the Van der Waals radii for nitrogen (1.55 Å) and iodine (1.98 Å) [31], but longer than the sum of the covalent radii for N (0.70 Å) and I (1.33 Å). These observations also provide evidence that all the tested N-containing heterocycles form intermolecular charge-transfer complexes with I_2. The smaller the I1–I2 distance, the more favorable complexation is. The N···I1–I2 bond angle is almost linear. Fig. 5 represents the correlation of the V_{oc} with the intermolecular N···I1 and the intramolecular I1–I2 atom distances in the complexes. The shorter N···I1 distance, the higher the V_{oc} value is. On the contrary, as the I1–I2 distance lengthens and becomes further from the isolated I_2 molecule one (dashed line in Fig. 5), the V_{oc} increases.

Fig. 6 shows the correlation of the V_{oc} with the stretching frequencies of the intermolecular N···I1 ($\nu_{N\cdots I1}$) and intramolecular I1–I2 (ν_{I1-I2}) bonds. Data pertinent to the intra- and intermolecular stretching degrees of freedom, I1–I2 and N···I1, which change the most in these complexes [32], is inspected. The σ*-orbital of iodine attracts electrons from the N lone pair (LP(N)) in a push–pull manner, which lengthens the intramolecular I1–I2 bond (see Fig. 5) from the monomer bond during complexation and the corresponding stretching

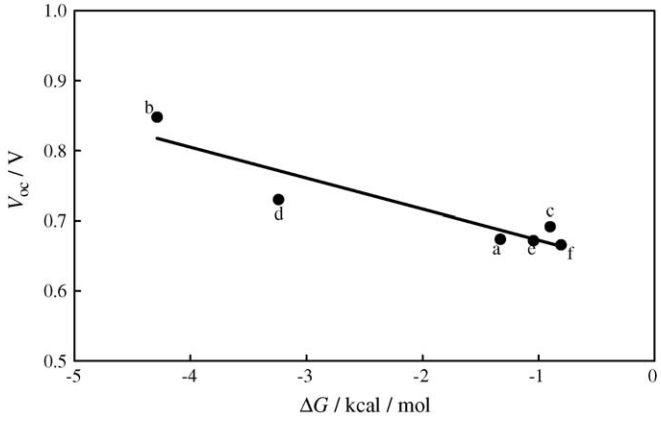

Fig. 3. Correlation between the V_{oc} and the ΔG of Eq. (1). The number of each molecule is defined in Table 1.

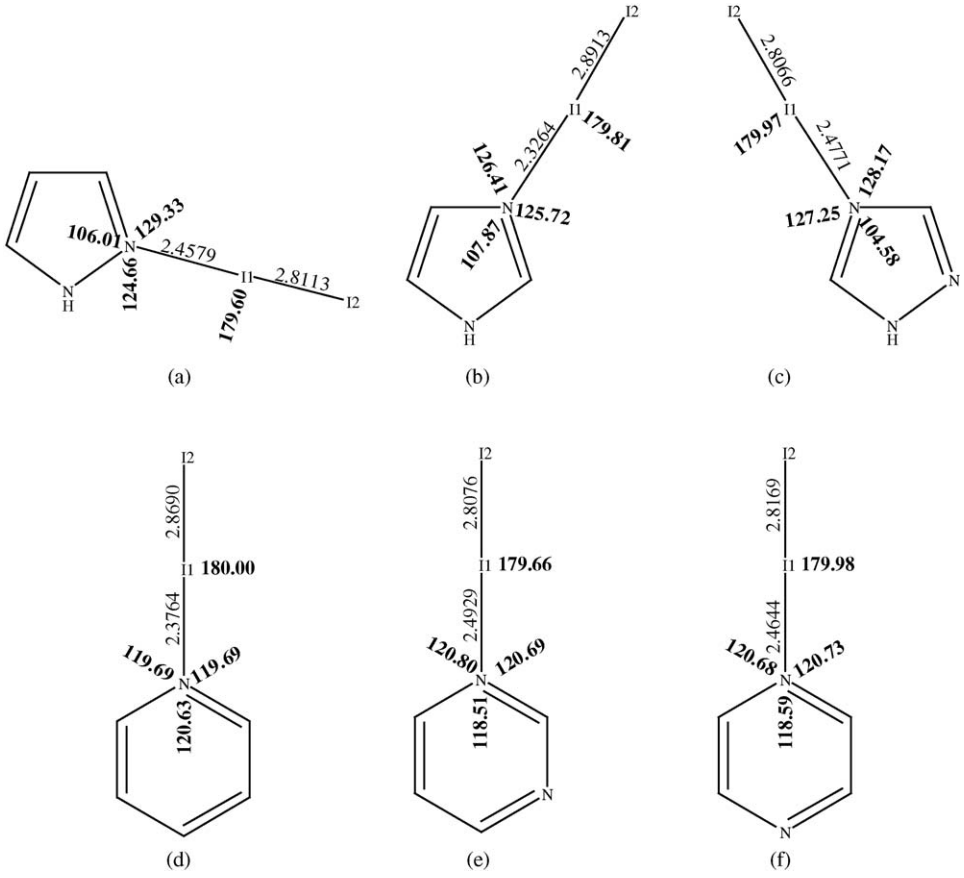

Fig. 4. Optimized geometries of (a) pyrazole, (b) imidazole, (c) 1,2,4-triazole, (d) pyridine, (e) pyrimidine, and (f) pyrazine complexes with I_2. Distances are in Ångström (normal letters) and the angles are in degrees (bold letters).

frequency decreases from the monomer as shown by $\nu_{I1–I2}$. The weakened bond and lower stretching vibration provide more evidence for complexation. The large gain in the stretching vibration of the acceptor bond leads to a stronger intermolecular charge-transfer complex [33]. On the contrary, when a stronger charge-transfer complex is formed, the larger the stretching frequency of the N···I1 bond ($\nu_{N\cdots I1}$). The V_{oc} increases as $\nu_{N\cdots I1}$ is blue-shifted, but $\nu_{I1–I2}$ is red-shifted as the value becomes further from the isolated I_2 molecule (220 cm^{-1}).

To understand further the nature and magnitude of the intermolecular interactions, NBO analysis was conducted on the optimized geometries in Fig. 4. To complete the span of the valence space in the NBO analysis [30], each valence bonding NBO (σ_{AB}) must be paired with the corresponding valence antibonding NBO (σ^*_{AB})

$$\sigma*_{AB} = c_A h_A - c_B h_B \quad (5)$$

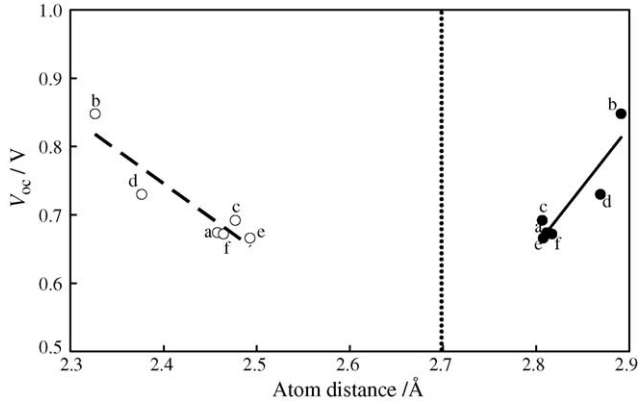

Fig. 5. Correlation of the V_{oc} with (◯) the intermolecular N···I1 atom distance and (●) the intramolecular I1–I2 atom distance of the complexes. The number of each complex is defined in Fig. 3.

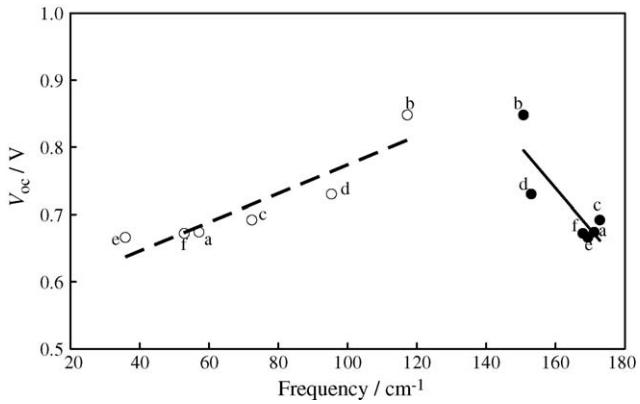

Fig. 6. Correlation of the V_{oc} with (◯) the N···I1 stretching frequencies ($\nu_{N\cdots I1}$) and (●) the I1–I2 stretching frequencies ($\nu_{I1–I2}$) of the complexes. The number of each complex is defined in Fig. 3.

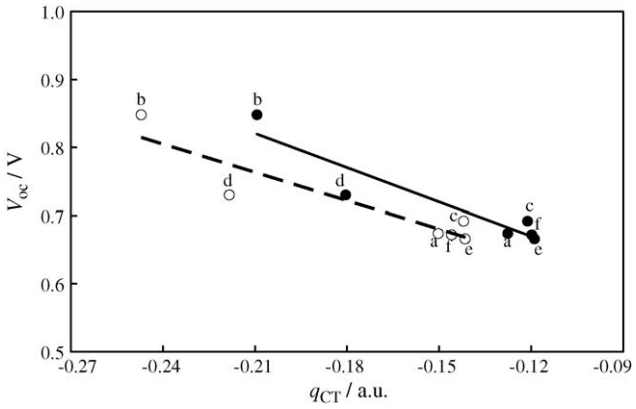

Fig. 7. Correlation of the V_{oc} with the net charge transferred (q_{CT}) for the complexes (◯) by Mulliken population analysis and (●) by NBO analysis. The number of each complex is defined in Fig. 3.

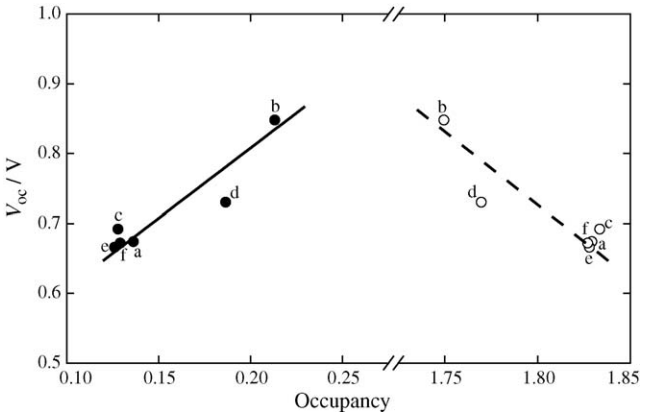

Fig. 8. Correlation of the V_{oc} with the occupancy of (◯) LP(N) and (●) σ*(I–I) for the complexes. The number of each complex is defined in Fig. 3.

Namely, in an ideal Lewis structure, the 'Lewis'-type (donor) NBOs are complemented by the 'non-Lewis'-type (acceptor) NBOs, which are formally empty. The general transformation to NBOs leads to unoccupied orbitals in the formal Lewis structure. Consequently, the filled NBOs of the natural Lewis structure accurately describe the covalency effects in these molecules. Since the non-covalent delocalization effects are associated with $\sigma \rightarrow \sigma^*$ interactions between the filled (donor) and unfilled (acceptor) orbitals, it is natural to describe them as 'donor–acceptor', charge transfer, or generalized 'Lewis base–Lewis acid' type interactions. The antibonds represent the unused valence-shell capacity and the spanning portions of the atomic valence space, which are formally unsaturated by covalent bond formation. The weak occupancies of the valence antibonds indicate irreducible departures from the ideal localized Lewis picture, i.e., true 'delocalization effects'.

Therefore, the donor–acceptor (bonding–antibonding) interactions in the NBO analysis are considered by examining all the possible interactions between the 'filled' (donor) Lewis-type NBOs and the 'empty' (acceptor) non-Lewis NBOs. Then their energies are estimated by the second-order perturbation theory. These interactions (or energetic stabilizations) are the 'delocalization' corrections to the zeroth-order natural Lewis structure. For each donor NBO (i) and acceptor NBO (j), the stabilization energy $E^{(2)}$, which is associated with the $i \rightarrow j$ delocalization, is estimated by Eq. (6):

$$E^{(2)} = \Delta E_{ij} = q_i \frac{F^2(i,j)}{\varepsilon_j - \varepsilon_i} \tag{6}$$

where q_i is the ith donor orbital occupancy. ε_i and ε_j are the diagonal elements (orbital energies), while $F(i, j)$ is the off-diagonal element associated with the NBO Fock matrix. Hence, the valence antibond (σ*) leads to a far-reaching extension of the elementary Lewis structure concept and achieves the delocalization corrections with simple NBO perturbative estimates using Eq. (6) [34]. In the charge-transfer complexation theory mentioned in Section 1, $E^{(2)}$ of the LP(N) → σ*(I–I) interaction corresponds the stabilization energy, Δ.

Fig. 7 illustrates the correlation of the V_{oc} with the net charge transferred (q_{CT}) [14] obtained from the Mulliken population and NBO analyses. Although the q_{CT} values determined by the Mulliken population analysis are larger than those by NBO one, the V_{oc} value increases with q_{CT}.

Fig. 8 depicts the correlation of the V_{oc} with the occupancies of the σ*(I–I) and the LP(N) for the heterocycle·I_2 complexes. These correlations indicate that the V_{oc} increases with the occupancy of the σ*(I–I), but decreases with that of the LP(N).

Fig. 9 illustrates the correlation between the V_{oc} and $E^{(2)}$ of the LP(N) → σ*(I–I) interaction in the complexes. The higher the $E^{(2)}$ value, the larger the V_{oc} of the solar cell.

All these correlations suggest that a higher V_{oc} is obtained when the N-containing heterocycles and I_2 form a more favorable intermolecular charge-transfer complex. The larger the intermolecular charge-transfer complexation and the lower the [I_3^-], the more efficiently the holes are collected [5,6] and/or the electron concentration in the TiO_2 film increases since recombination of the electron with electrolyte (Fig. 1(5)) is suppressed [2,6,7], which leads to a higher V_{oc}. Moreover, complexation between the heterocycles and I_2 may prevent the loss of the thiocyanato ligand (SCN^-), which is believed to be important

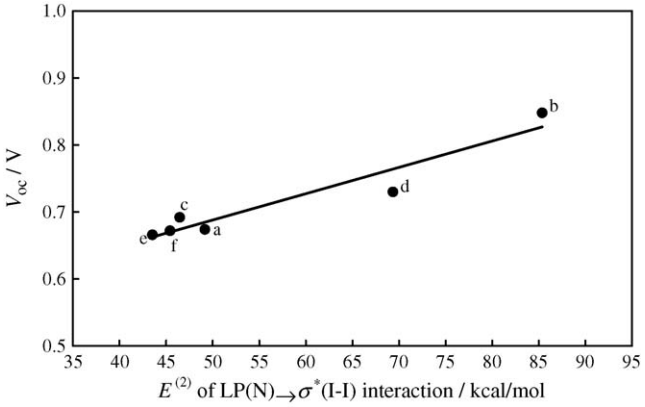

Fig. 9. Correlation between the V_{oc} and the second-order perturbation energy ($E^{(2)}$) of the LP(N) → σ*(I–I) interaction in the complexes. The number of each complex is defined in Fig. 3.

in the reduction of the oxidized dye to regenerate the original N719 dye (Fig. 1(7)):

$$(\text{dcbpy})_2\text{Ru(SCN)}_2^{2-} + 2\text{I}_3^- \rightleftarrows (\text{dcbpy})_2\text{RuI}_2^{2-} + 2\text{I}_2\text{SCN}^- \quad (7)$$

Eq. (1) will cause equilibrium (7) to move to the left [7]. Therefore, the theoretical calculations confirm that the intermolecular charge-transfer complexation between the N-containing heterocyclic additives and I_2 in the I^-/I_3^- redox electrolyte in acetonitrile greatly influences the V_{oc} in a Ru(II) complex dye-sensitized TiO_2 solar cell.

Comparing the calculation results of isomers indicates that the intermolecular interaction in imidazole·I_2 is stronger than that in pyrazole·I_2. For azine isomers, I_2 prefers the pyrazine complex to the pyrimidine one. These observations are consistent with the V_{oc} trends mentioned above.

4. Conclusion

Ab initio MO computational calculations were used to theoretically investigate the monomer and intermolecular 1:1 charge-transfer complexes of six different N-containing heterocycles with I_2 where the σ* orbital of I–I and the N lone pair in the heterocycles interact. The computational results were compared to the V_{oc} values observed for a Ru(II) complex dye-sensitized nanocrystalline TiO_2 solar cell using these heterocyclic additives in an I^-/I_3^- redox electrolyte solution. It was determined that the more negative the change in Gibbs free energy, the higher the V_{oc} of the cell is. Also, the shorter the intermolecular N···I distance in the complex, the more the V_{oc} is enhanced. Furthermore, the longer the intramolecular I–I distance, the higher the V_{oc} value. As the N···I stretching frequency is blue-shifted and the I–I is red-shifted, the V_{oc} of the cell increased. The V_{oc} value also increased with a net charge transferred. The V_{oc} increased as the lone pair occupancy of the N atom decreased and as the σ* occupancy of the I–I bond increased. The higher the stabilization energy for the LP(N) → σ*(I–I) interaction, the larger the V_{oc}. These correlations suggest that a more favorable intermolecular charge-transfer interaction occurs between the N-containing heterocycles and I_2 molecules when the V_{oc} value is higher. A dominant factor in determining the dye-sensitized solar cell performance is the intermolecular charge-transfer interaction between the additive donor and electrolyte acceptor.

References

[1] B. O'Reganoulos, M. Grätzel, Nature 353 (1991) 737–740.
[2] S.Y. Huang, G. Schlichthörl, A.J. Nozik, M. Grätzel, A.J. Frank, J. Phys. Chem. B 101 (1997) 2576–2582.
[3] G. Schlichthörl, S.Y. Huang, J. Sprague, A.J. Frank, J. Phys. Chem. B 101 (1997) 8141–8155.
[4] H. Kusama, M. Kurashige, H. Arakawa, J. Photochem. Photobiol. A: Chem. 169 (2005) 169–176.
[5] M. Grätzel, Nature 414 (2001) 338–344.
[6] J. He, G. Benkö, F. Korodi, T. Polívka, R. Lomoth, B. Åkermark, L. Sun, A. Hagfeldt, V. Sundström, J. Am. Chem. Soc. 124 (2002) 4922–4932.
[7] H. Greijer, J. Lindgren, A. Hagfeldt, J. Phys. Chem. B 105 (2001) 6314–6320.
[8] K. Ohno, Ryoshi Butsuri Kagaku, University of Tokyo Press, Tokyo, 1989, pp. 311–312.
[9] M.T. El-Haty, Spectrochim. Acta 47A (1991) 1017–1021.
[10] A.A.A.A. Boraei, O.M. El-Roudi, Can. J. Appl. Spectrosc. 41 (1996) 37–41.
[11] A.A.A.A. Boraei, Can. J. Appl. Sci. Spectrosc. 46 (2001) 95–100.
[12] G.A. Bowmaker, P.D.W. Boyd, J. Chem. Soc. Faraday Trans. 2 (83) (1987) 2211–2223.
[13] Y. Danten, B. Guillot, Y. Guissani, J. Chem. Phys. 96 (1992) 3795–3810.
[14] S. Reilling, M. Besnard, P.A. Bopp, J. Phys. Chem. A 101 (1997) 4409–4415.
[15] M.J. Frisch, G.W. Trucks, H.B. Schlegel, G.E. Scuseria, M.A. Robb, J.R. Cheeseman, J.A. Montgomery, Jr., T. Vreven, K.N. Kudin, J.C. Burant, J.M. Millam, S.S. Iyengar, J. Tomasi, V. Barone, B. Mennucci, M. Cossi, G. Scalmani, N. Rega, G.A. Petersson, H. Nakatsuji, M. Hada, M. Ehara, K. Toyota, R. Fukuda, J. Hasegawa, M. Ishida, T. Nakajima, Y. Honda, O. Kitao, H. Nakai, M. Klene, X. Li, J.E. Knox, H.P. Hratchian, J.B. Cross, V. Bakken, C. Adamo, J. Jaramillo, R. Gomperts, R.E. Stratmann, O. Yazyev, A.J. Austin, R. Cammi, C. Pomelli, J.W. Ochterski, P.Y. Ayala, K. Morokuma, G.A. Voth, P. Salvador, J.J. Dannenberg, V.G. Zakrzewski, S. Dapprich, A.D. Daniels, M.C. Strain, O. Farkas, D.K. Malick, A.D. Rabuck, K. Raghavachari, J.B. Foresman, J.V. Ortiz, Q. Cui, A.G. Baboul, S. Clifford, J. Cioslowski, B.B. Stefanov, G. Liu, A. Liashenko, P. Piskorz, I. Komaromi, R.L. Martin, D.J. Fox, T. Keith, M.A. Al-Laham, C.Y. Peng, A. Nanayakkara, M. Challacombe, P.M.W. Gill, B. Johnson, W. Chen, M.W. Wong, C. Gonzalez, J.A. Pople, Gaussian 03, Revision C.02, Gaussian, Inc., Wallingford CT, 2004.
[16] T.H. Dunning Jr., P.J. Hay, in: H.F. Schaefer III (Ed.), Modern Theoretical Chemistry, vol. 3, Plenum, New York, 1976, pp. 1–28.
[17] P.J. Hay, W.R. Wadt, J. Chem. Phys. 82 (1985) 270–283.
[18] W.R. Wadt, P.J. Hay, J. Chem. Phys. 82 (1985) 284–298.
[19] P.J. Hay, W.R. Wadt, J. Chem. Phys. 82 (1985) 299–310.
[20] M.W. Wong, P.M.W. Gill, R.H. Nobes, L. Radom, J. Phys. Chem. 92 (1988) 4875–4880.
[21] A.E. Reed, L.A. Curtiss, F. Weinhold, Chem. Rev. 88 (1988) 899–926.
[22] W. Schneider, W. Thiel, J. Chem. Phys. 86 (1987) 923–936.
[23] E. Cancès, B. Mennucci, J. Tomasi, J. Chem. Phys. 107 (1997) 3032–3041.
[24] M. Esseffar, W. Bouab, A. Lamsabhi, J.L.M. Abboud, R. Notario, M. Yáñez, J. Am. Chem. Soc. 122 (2000) 2300–2308.
[25] A. El Firdoussi, M. Esseffar, W. Bouab, J.-L.M. Abboud, O. Mó. M. Yáñez, J. Phys. Chem. A 108 (2004) 10568–10577.
[26] S.P. Ananthavel, M. Manoharan, Chem. Phys. 269 (2001) 49–57.
[27] B. Mennucci, R. Cammi, J. Tomasi, J. Chem. Phys. 109 (1998) 2798–2807.
[28] J. Tomasi, B. Mennucci, E. Cancès, J. Mol. Struct. (Theochem.) 464 (1999) 211–226.
[29] J.P. Foster, F. Weinhold, J. Am. Chem. Soc. 102 (1980) 7211–7218.
[30] E.D. Glendening, A.E. Reed, J.E. Carpenter, F. Weinhold, NBO Version 3.1.
[31] A. Bondi, J. Phys. Chem. B 68 (1964) 441–451.
[32] A. Karpfen, J. Phys. Chem. A 105 (2001) 2064–2072.
[33] Y. Zhang, X.-Z. You, J. Comput. Chem. 22 (2001) 327–338.
[34] A. Ebrahimi, F. Deyhimi, H. Roohi, J. Mol. Struct. (Theochem.) 626 (2003) 223–229.